Gid10 as an alternative N-recognin of the Pro/N-degron pathway

Artem Melnykov[a], Shun-Jia Chen[a], and Alexander Varshavsky[a,1]

[a]Division of Biology and Biological Engineering, California Institute of Technology, Pasadena, CA 91125

Contributed by Alexander Varshavsky, June 6, 2019 (sent for review May 14, 2019; reviewed by Wolfgang Baumeister and Avram Hershko)

In eukaryotes, N-degron pathways (formerly "N-end rule pathways") comprise a set of proteolytic systems whose unifying feature is their ability to recognize proteins containing N-terminal degradation signals called N-degrons, thereby causing degradation of these proteins by the 26S proteasome or autophagy. Gid4, a subunit of the GID ubiquitin ligase in the yeast *Saccharomyces cerevisiae*, is the recognition component (N-recognin) of the GID-mediated Pro/N-degron pathway. Gid4 targets proteins by recognizing their N-terminal Pro residues or a Pro at position 2, in the presence of distinct adjoining sequence motifs. Under conditions of low or absent glucose, cells make it through gluconeogenesis. When *S. cerevisiae* grows on a nonfermentable carbon source, its gluconeogenic enzymes Fbp1, Icl1, Mdh2, and Pck1 are expressed and long-lived. Transition to a medium containing glucose inhibits the synthesis of these enzymes and induces their degradation by the Gid4-dependent Pro/N-degron pathway. While studying yeast Gid4, we identified a similar but uncharacterized yeast protein (YGR066C), which we named Gid10. A screen for N-terminal peptide sequences that can bind to Gid10 showed that substrate specificities of Gid10 and Gid4 overlap but are not identical. Gid10 is not expressed under usual (unstressful) growth conditions, but is induced upon starvation or osmotic stresses. Using protein binding analyses and degradation assays with substrates of GID, we show that Gid10 can function as a specific N-recognin of the Pro/N-degron pathway.

Gid10 | Gid4 | Fbp1 | ubiquitin | degradation

Cellular proteolytic systems mediate selective destruction of misfolded, aggregated, and otherwise abnormal proteins, and also regulate the levels of proteins that evolved to be short-lived in vivo. Proteins that fold too slowly, misfold, or do not satisfy other requirements of quality control, are also selectively eliminated. Two multithreaded mechanisms, the ubiquitin (Ub)-proteasome system (UPS) and autophagy-lysosome pathways, mediate the bulk of intracellular protein degradation, with molecular chaperones playing specific roles in both systems (1–20).

The UPS consists of pathways that have in common at least 2 kinds of enzymes: Ub ligases (E2-E3 enzymes) and deubiquitylases (DUBs). Proteins are recognized by a Ub ligase through their cognate degradation signals (degrons). In the next step, a Ub ligase conjugates the 9-kDa protein Ub to an amino acid residue of a targeted substrate (usually an internal Lys residue), forming, in most cases, a substrate-linked poly-Ub chain. The functions of DUBs include deubiquitylation of Ub-conjugated proteins (2, 9, 11, 21–27). The 26S proteasome, a multisubunit ATP-dependent protease, recognizes a substrate-linked poly-Ub chain, binds to it, and unfolds the target protein through activities of proteasome's ATPases. The target protein is then processively destroyed by the protease part of the 26S proteasome, yielding short (~10-residue) peptides (20, 28–35).

N-degron pathways (previously called "N-end rule pathways") are a set of proteolytic systems whose unifying feature is their ability to recognize proteins containing N-terminal (Nt)-degradation signals called N-degrons, thereby causing the degradation of these proteins by the 26S proteasome and/or autophagy in eukaryotes, and by the proteasome-like ClpAP protease in bacteria (2, 20, 25, 36–75). (N-degron pathways are Ub-dependent in eukaryotes but not in bacteria.) The main determinants of an N-degron comprise a destabilizing Nt-residue of a protein substrate, an internal Lys residue (or residues) that acts as the site of polyubiquitylation, and a conformationally disordered region that mediates the start of processive degradation (2, 37).

Initially, most N-degrons are pro-N-degrons. They are converted to active N-degrons either constitutively (e.g., during the emergence of a protein from a ribosome) or conditionally, via regulated steps. Among the routes to N-degrons are cleavages of proteins by nonprocessive proteases (e.g., by caspases, calpains, separases, or aminopeptidases) that act as initial targeting components of N-degron pathways by cleaving a prosubstrate protein and generating a destabilizing neo-Nt-residue in a resulting C-terminal (Ct) fragment (20, 40, 57, 70, 71, 76–81). A different and mutually nonexclusive route to N-degrons is through enzymatic Nt-modifications of proteins, including Nt-acetylation, Nt-deamidation, Nt-arginylation, Nt-leucylation, or Nt-formylation of Nt-residues. Recognition components of N-degron pathways, called N-recognins, are E3 Ub ligases or other proteins (e.g., bacterial ClpS or mammalian p62) that can target specific N-degrons (2, 14, 41). In cognate sequence contexts, all 20 amino acids of the genetic code can act as destabilizing Nt-residues (Fig. 1). Consequently, a number of cellular proteins (and their protease-generated Ct-fragments as well) are either constitutively or conditionally short-lived N-degron substrates.

Eukaryotic N-degron pathways comprise the Arg/N-degron pathway (it recognizes, in particular, specific unacetylated Nt-residues); the Ac/N-degron pathway (it recognizes, in particular, the N^{α}-terminally acetylated [Nt-acetylated] Nt-residues); the

Significance

In eukaryotes, N-degron pathways comprise proteolytic systems whose unifying feature is their ability to recognize proteins containing N-terminal degradation signals called N-degrons, thereby causing degradation of these proteins. Gid4, a subunit of the GID ubiquitin ligase in the yeast *Saccharomyces cerevisiae*, is the recognition component (N-recognin) of the Pro/N-degron pathway. Gid4 targets proteins by recognizing their N-terminal Pro residues or a Pro at position 2. We identified an uncharacterized Gid4-like yeast protein, termed Gid10. A screen for N-terminal sequence motifs that can bind to Gid10 showed that substrate specificities of Gid10 and Gid4 overlap but are not identical. We also found that Gid10 can function as a specific N-recognin of the GID ubiquitin ligase and the Pro/N-degron pathway.

Author contributions: A.M., S.-J.C., and A.V. designed research; A.M. and S.-J.C. performed research; A.M., S.-J.C., and A.V. analyzed data; and A.M., S.-J.C., and A.V. wrote the paper.

Reviewers: W.B., Max Planck Institute of Biochemistry; and A.H., Technion Israel Institute of Technology.

The authors declare no conflict of interest.

[1]To whom correspondence may be addressed. Email: avarsh@caltech.edu.

This article contains supporting information online at www.pnas.org/lookup/suppl/doi:10.1073/pnas.1908304116/-/DCSupplemental.

Published online July 23, 2019.

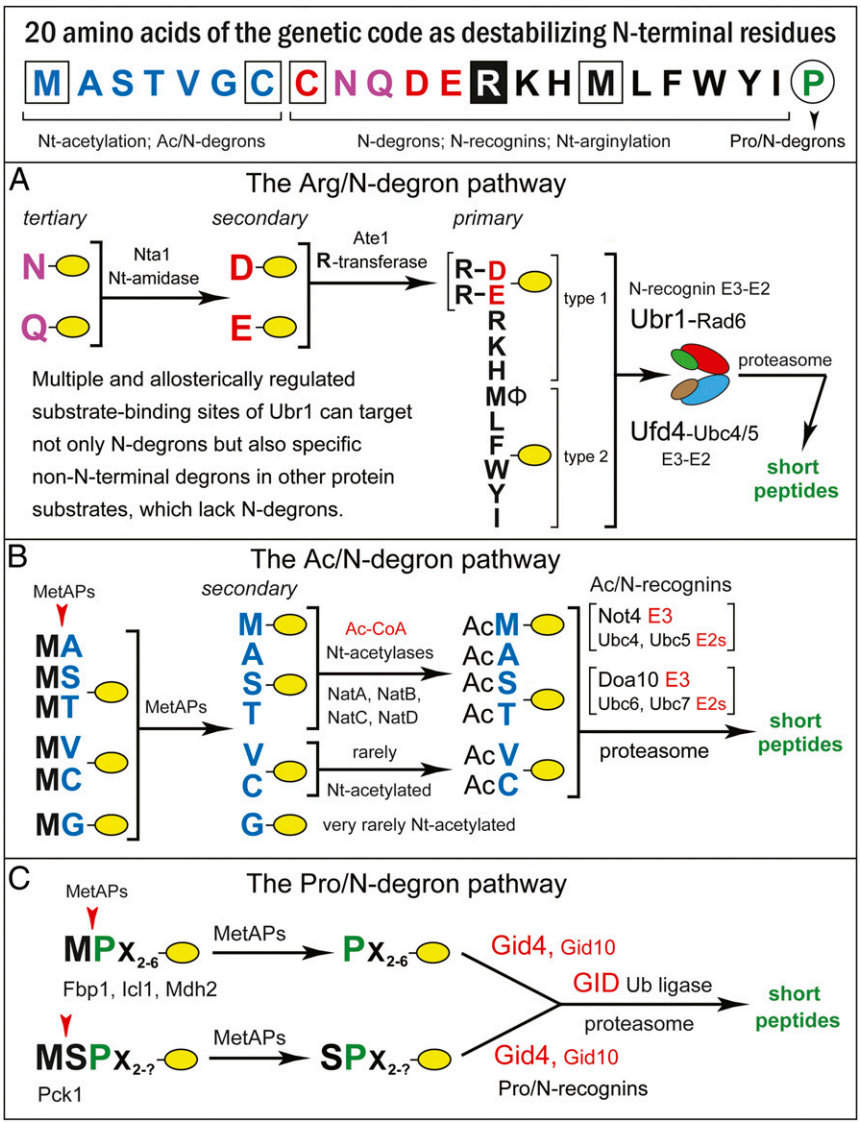

Fig. 1. N-degron pathways. Nt-residues at the *Top* of the diagram are indicated by single-letter abbreviations. Twenty DNA-encoded amino acids are arranged to delineate 3 sets of N-degrons in *S. cerevisiae*, corresponding to 3 N-degron pathways. Nt-Met is cited twice, because it can be recognized by the Ac/N-degron pathway (as the Nt-acetylated Nt-Met) and by the Arg/N-degron pathway (as the unacetylated Nt-Met). Nt-Cys is also cited twice, because it can be recognized by the Ac/N-degron pathway (as Nt-acetylated Nt-Cys) and by the Arg/N-degron pathway (as an oxidized, Nt-arginylatable Nt-Cys, which is formed in multicellular eukaryotes but apparently not in unstressed *S. cerevisiae*). (*A*) The Arg/N-degron pathway. (*B*) The Ac/N-degron pathway. (*C*) The Pro/N-degron pathway. The diagram indicates both Gid4, the main Pro/N-recognin, and Gid10, the pathway's alternative Pro/N-recognin that has been analyzed in the present study. The fourth eukaryotic pathway, termed the fMet/N-degron pathway, is described in ref. 50. See Introduction for references and brief descriptions of these pathways.

Pro/N-degron pathway (it recognizes, in particular, the Nt-Pro residue or a Pro at position 2, in the presence of distinct adjoining sequence motifs); and the fMet/N-degron pathway (it recognizes Nt-formylated cellular proteins) (Fig. 1) (2, 20, 38, 41–45).

Regulated degradation of proteins and their natural fragments by N-degron pathways (Fig. 1) has been shown to mediate a multitude of processes, including the sensing of heme, oxygen, and nitric oxide; the control of subunit stoichiometries in protein complexes; the elimination of misfolded proteins and of proteins retrotranslocated to the cytosol from other compartments; the repression of neurodegeneration and regulation of apoptosis; the regulation of DNA repair, transcription, replication, and chromosome cohesion/segregation; the regulation of chaperones, G proteins, cytoskeletal proteins, autophagy, gluconeogenesis, peptide import, meiosis, circadian rhythms, fat metabolism, cell migration, immunity (including inflammation), the cardiovascular system, spermatogenesis, and neurogenesis; and the regulation of many processes in plants (refs. 2, 20, 25, 38, and 40–75 and refs. therein).

Under conditions of low or absent glucose, the yeast *Saccharomyces cerevisiae* and other eukaryotes synthesize it through gluconeogenesis. In yeast, the main gluconeogenesis-specific cytosolic enzymes are the Fbp1 fructose-1,6-bisphosphatase, the Icl1 isocitrate lyase, the Mdh2 malate dehydrogenase, and the Pck1 phosphoenolpyruvate carboxykinase (20, 46, 82–95). When *S. cerevisiae* (*Sc*) grows on a nonfermentable carbon source such as, e.g., ethanol, gluconeogenic enzymes are expressed and long-lived. Transition to a medium containing glucose inhibits the synthesis of these enzymes and induces their degradation. As shown by Wolf, Chiang and colleagues, under experimental conditions encompassed in the present study, the degradation of yeast gluconeogenic enzymes is mediated by the multisubunit GID Ub ligase and the 26S proteasome (20, 86, 87, 90, 96, 97).

A notable aspect of GID-mediated processes is the dichotomy between the GID/proteasome-mediated degradation of gluconeogenic enzymes and the "alternative" degradation of these enzymes through an autophagy-related pathway called vacuolar import and degradation (VID) (87, 90, 93, 95, 98–100). The VID pathway may also involve a GID-mediated polyubiquitylation of gluconeogenic enzymes. Whether these enzymes are destroyed (after a return of yeast cells to glucose-containing media) largely by the GID/proteasome pathway or largely by the VID pathway depends, among other things, on the duration of glucose starvation and the nature of a nonglucose carbon source (84, 101). The functions of this remarkable dichotomy, the regulation of transitions

between the GID/proteasome and VID pathways, and molecular mechanisms of VID remain to be understood (46, 96).

The *S. cerevisiae* 41-kDa Gid4 is a subunit of the GID Ub ligase that is conserved from yeast to mammals. Our previous work has shown that Gid4 is the N-recognin of the GID-mediated proteolytic system termed the Pro/N-degron pathway (Fig. 1C) (46). Gid4 was shown to recognize a protein substrate through its Nt-Pro residue or a Pro at position 2, in the presence of distinct adjoining sequence motifs (46, 48). The *S. cerevisiae* gluconeogenic enzymes Fbp1, Icl1, Mdh2, and Pck1 bear either Nt-Pro (Fbp1, Icl1, Mdh2) or a Pro at position 2 (Pck1), and are conditionally short-lived substrates of the Gid4-dependent Pro/N-degron pathway (Fig. 1C) (46, 48).

The crystal structure of human Gid4, recently determined by Min and colleagues (47, 48), comprises an antiparallel β-barrel that contains a deep and narrow substrate-binding cleft. The substrate specificity of human Gid4, characterized through in vitro binding assays with synthetic peptides (47), is similar to the specificity of *S. cerevisiae* Gid4 that has been analyzed using in vivo 2-hybrid (Y2H) assays (46). In mammals, the GID (also called CTLH) Ub ligase has been shown to play a role in cell proliferation, in the functioning of primary cilia, and in other processes (96, 102–111). Mammalian proteins that contain Pro/N-degrons and are targeted for degradation by the mammalian Gid4 N-recognin remain to be identified.

The ~600-kDa *S. cerevisiae* GID Ub ligase comprises at least the Gid1, Gid2, Gid4, Gid5, Gid7, Gid8, and Gid9 subunits, in addition to the weakly associated Ubc8 (Gid3) E2 (Ub-conjugating) enzyme (46, 86, 96). While studying yeast Gid4, we found that an uncharacterized *S. cerevisiae* protein encoded by the ORF *YGR066C* is significantly sequelogous (112) (similar in sequence) to Gid4: 52% similar, 33% identical (Fig. 2*A*). Given this level of sequelogy between Gid4 and the previously uncharacterized YGR066C (Fig. 2*A*), we provisionally termed the latter protein Gid10, and proceeded to analyze it.

["Sequelog" denotes a sequence that is similar, to a specified extent, to another sequence (112). Derivatives of "sequelog" include "sequelogous" (similar in sequence) and "sequelogy" (sequence similarity). The usefulness of "sequelog" and derivative notations stems from the clarity and rigor of their evolutionary neutrality. In contrast, "homolog," "ortholog," and "paralog," which invoke, respectively, common descent and functional similarity/dissimilarity, are often imprecise, interpretation-laden terms. The sequelog terminology is compatible with homolog/ortholog/paralog. The latter terms can be used to convey an understanding about common descent and biological functions, if this information (it is distinct from sequence similarities per se) is actually present (112).]

We found that the 34-kDa *S. cerevisiae* Gid10 is a conditionally expressed subunit of the GID Ub ligase that is functionally similar to the Gid4 (N-recognin) subunit. The substrate specificities of Gid10 and Gid4 (surveyed through a genetic screen) overlap but are not identical. We traced the evolution of Gid10 among budding yeasts. *S. cerevisiae* Gid10 is not expressed under usual (unstressful) growth conditions, but is induced upon starvation or osmotic stresses. Using protein substrates of GID, degradation assays, and protein binding analyses, we also show that Gid10 can function as a specific N-recognin of the Pro/N-degron pathway.

Results and Discussion

A Screen for N-Terminal Motifs That Bind to Gid10. This screen employed the yeast-based Y2H technique (46, 113–115) to detect interactions between *S. cerevisiae* Gid10 and short (~4 residues) N-terminal sequence motifs. A Y2H-based Gid10 construct

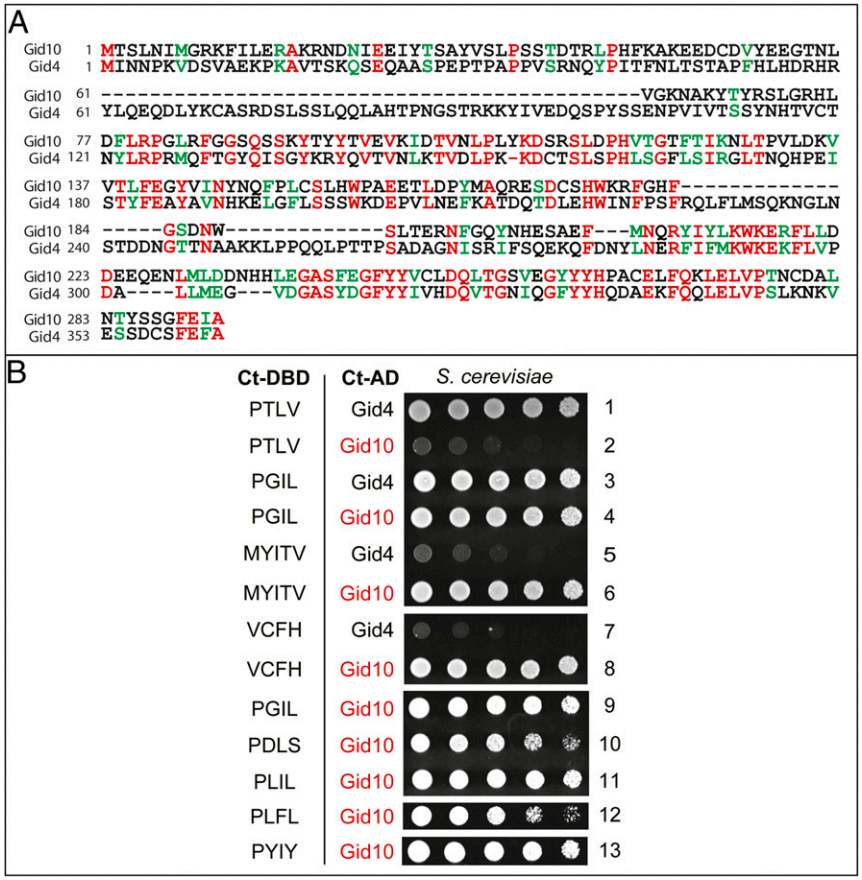

Fig. 2. Sequelogy between *S. cerevisiae* Gid4 and Gid10 (Ygr066c), and the binding of these proteins to specific Nt-polypeptide segments. (*A*) Alignment of Gid4 and Gid10 amino acid sequences. Identical residues are in red. Dissimilar residues are in black. Similar residues are in green. The residues of (aligned) Gid4 and Gid10 were classed as similar if they were both basic, or both acidic, or both amides, or both hydrophobic (defined as all hydrophobic residues in the set of 20 amino acids, save for Ala, Cys, and Gly), or, with Ser and Thr, both uncharged/hydrophilic. (*B*) Two-hybrid (Y2H) binding assays with Gid4 and Gid10 vs. specific Nt-sequences, which are indicated on the *Left* using single-letter abbreviations for amino acids. With the exception of Nt-PTLV (the first 4 residues of wild-type *S. cerevisiae* Fbp1) (46), all indicated Nt-sequences were identified through the Y2H-based genetic screen (see *Results and Discussion*). Note the absence of a significant binding of Gid10 (but not Gid4) to Nt-PTLV, and the opposite binding pattern with (at least) the Nt-sequences Nt-MYITV and Nt-VCFH. Ct-AD and Ct-DBD denote Y2H-specific protein domains linked to test proteins (see *Materials and Methods*).

comprised a fusion of Gid10 to a Ct-segment containing the yeast Gal4 transcription activation domain (AD). The other component of the screen was a PCR-generated library of $MX_2X_3X_4X_5$-GGGGGG-Dhfr-DBD fusions, in which the last (Ct) segment was the Gal4 DNA-binding domain (DBD). "M" (in single-letter amino acid abbreviations) denotes the Nt-Met residue of a Y2H fusion. $X_2X_3X_4X_5$ denotes a quasirandom 4-residue sequence, encoded by a PCR-generated DNA segment. That (randomized) sequence was followed by the Gly_6 linker segment, the 21-kDa moiety of the mouse dihydrofolate reductase (Dhfr), and the DBD domain. An in vivo interaction of the Gid10 protein with an Nt-sequence from the library would induce the *HIS3* reporter gene, thereby making it possible to detect an interaction by selecting for growth of Y2H yeast strains on a medium without histidine (Fig. 2*B*) (see *Materials and Methods*).

Binding Specificities of Gid10 vs. Gid4. The screen identified several Nt-sequences that bound to Gid10 tightly enough to be robustly detected by Y2H assays (Fig. 2*B*, rows 4, 6, and 8 through 13). The Nt-Met residue is cotranslationally removed from a nascent polypeptide if a residue at position 2, to be made N-terminal upon the cleavage, is either Pro, Gly, Ala, Cys, Ser, Thr, or Val. Residues at position 2 that are larger than Val would be made N-terminal either much more slowly or not at all (116, 117). Some Gid10-binding Nt-sequences were found to contain proline (Pro) at the X_2 position. (As described above, the Pro-occupied position X_2 would become N-terminal in vivo.) The Nt-Pro aspect of the binding specificity of Gid10 resembled the previously characterized (46) binding specificity of Gid4 (Fig. 1*C*). For example, we found that the Nt-sequence PGIL (in single-letter amino acid notations), which was identified through the above screen, was bound by Gid4 and Gid10 approximately equally strongly in Y2H assays (Fig. 2*B*, rows 3, 4, and 9). These and other results, including degradation assays (see below), indicated that Gid10 was, in fact, an N-recognin analogous to Gid4.

The Y2H-based screen also showed that the binding specificities of Gid4 and Gid10 could be distinct. For example, Gid10 did not significantly interact, in Y2H assays, with Nt-PTLV, the Nt-sequence of the *S. cerevisiae* gluconeogenic enzyme Fbp1. In contrast, Nt-PTLV bound to Gid4, and the binding required the Nt-Pro residue of PTLV (Fig. 2*B*, rows 1 and 2). Through its recognition of the Nt-PTLV sequence of Fbp1, Gid4 mediates the degradation of Fbp1 upon a transition from growth on ethanol to growth on glucose (46). Another difference between interactions of Gid10 and Gid4 with Nt-sequences involved a significant preference, by Gid10, for a hydrophobic residue after the Nt-Pro residue (Fig. 2*B*).

An even stronger difference between the binding specificities of Gid10 vs. Gid4 was exemplified by other Gid10-positive hits from the Y2H library that have been examined, in addition, for their binding to Gid4. These sequences included Nt-MYITV and Nt-VCFH [in the former Nt-sequence, Nt-Met was retained in vivo (116, 117)] (Fig. 2*B*, rows 5 through 8). Although neither one of these Gid10-binding sequences contained a Pro residue, they robustly bound to Gid10, but did not significantly bind to Gid4 (Fig. 2*B*, rows 5 through 8). In sum, the sequelogous Gid10 and Gid4 (Fig. 2*A*) can recognize (bind to) the same Nt-sequences (one example is Nt-PGIL), but can also exhibit different specificities, with Gid10 (but not Gid4) recognizing Nt-MYITV and Nt-VCFH, and with Gid4 (but not Gid10) recognizing Nt-PTLV, the natural Nt-sequence of Fbp1, a physiological substrate of the Pro/N-degron pathway (Fig. 2*B*, rows 1, 2, and 5 through 8) (46).

Gid10 as a Functional Analog of the Gid4 N-Recognin. Our initial assessments indicated that *GID10* mRNA was virtually absent in *S. cerevisiae* under conditions of exponential growth on standard media. To determine whether Gid10, if it were ectopically expressed in yeast cells, might function as an N-recognin analogous to Gid4, we constructed a [*gid4Δ* P_{GID4}-*GID10*] strain, which contained 2 alterations: the *GID10* gene was deleted, and the *GID4* ORF was replaced with the *GID10* ORF, downstream from the natural P_{GID4} transcriptional promoter. As a result, Gid10 would be ectopically expressed (in cells that lacked the Gid4 protein) in patterns similar to those of Gid4. Other *S. cerevisiae* strains constructed for these assays included [*gid4Δ gid10Δ*] (lacking both *GID4* and *GID10*); [*gid4Δ gid2Δ*] (lacking *GID4* and also *GID2*, an essential subunit of the GID Ub ligase) (117); and *gid10Δ* (lacking *GID10* but containing *GID4*).

For experiments described in Fig. 3, yeast cells were grown to midexponential phase, with glucose as the carbon source. As shown previously, the endogenous Gid4 Pro/N-recognin was expressed and sufficiently active under these conditions to mediate the degradation of (at least) the Fbp1, Mdh2, and Icl1 gluconeogenic enzymes (46). Protein degradation was assayed using the promoter reference technique (PRT) (20). In this method, both a protein of interest and a long-lived reference protein (a dihydrofolate reductase) (Dhfr) are expressed in *S. cerevisiae* from the same plasmid, from identical constitutive promoters that contain additional DNA elements. Once transcribed, these elements form 5′-RNA aptamers that can bind to the added tetracycline (Tc). As a result, Tc, which does not affect global translation in the cytosol, can selectively repress translation of the aptamer-containing mRNAs that encoded the reference and the test proteins (20). Advantages of PRT include a built-in, accuracy-increasing reference protein as well as avoidance of cytotoxic, artifact-prone global translation inhibitors in chase-degradation assays (20). Following the addition of Tc, a decrease, during a chase, in the amount of a test protein relative to the reference protein would signify degradation of the test protein.

We wished our first test protein to be recognized by both Gid10 and Gid4. Therefore, the wild-type (WT) yeast Fbp1 was modified by replacing its first 4 residues (PTLV) with PGIL, an Nt-sequence (identified through the Y2H-based screen) (Fig. 2*B*, rows 3 and 4) that interacted with both Gid10 and Gid4. (In contrast, only Gid4, but not Gid10, significantly interacted with the Nt-PTLV sequence of WT Fbp1; Fig. 2*B*, rows 1 and 2.) The resulting test protein, C-terminally triple ha-tagged, was denoted as pgil-$Fbp1_{3ha}$, with the Nt-sequence "pgil" in lowercase, to avoid confusion vis-à-vis an uppercase letter in the rest of the protein's name.

The pgil-$Fbp1_{3ha}$ protein was long-lived in [*gid4Δ gid10Δ*] cells that lacked both Gid4 and Gid10, but short-lived in *gid10Δ* cells that lacked Gid10 and contained the Gid4 Pro/N-recognin, indicating that Gid4 could target pgil-$Fbp1_{3ha}$ for degradation (Fig. 3 *A* and *F*). Tellingly, pgil-$Fbp1_{3ha}$ protein was also short-lived in [*gid4Δ* P_{GID4}-*GID10*] cells, which lacked Gid4 and ectopically expressed Gid10 (Fig. 3 *A* and *F*). The latter and crucial result indicated that Gid10 was a functionally active N-recognin that could bind to pgil-$Fbp1_{3ha}$ similarly to Gid4 and could couple that recognition to the degradation of pgil-$Fbp1_{3ha}$ by the GID-mediated Pro/N-degron pathway.

Analogous PRT-based chase-degradation assays were carried out with myitv-$Fbp1_{3ha}$, in which the PTLV Nt-sequence of WT Fbp1 was replaced by Nt-MYITV. This Nt-sequence was identified through the Y2H-based screen as one of the Nt-sequence motifs that interacted with Gid10 but did not significantly interact with Gid4 (in contrast, Nt-PGIL interacted with both Gid10 and Gid4) (Fig. 2*B*, rows 3 through 6). As shown in Fig. 3 *B* and *G*, myitv-$Fbp1_{3ha}$ was degraded by the (ectopically) expressed Gid10, in a Gid4-lacking strain. In contrast, and in agreement with the absence of detectable Gid4 binding to Nt-MYITV, the stability of myitv-$Fbp1_{3ha}$ was essentially the same either in Gid4-containing (but Gid10-lacking) *gid10Δ* cells or in double-mutant [*gid4Δ gid10Δ*] cells (Fig. 3 *B* and *G*).

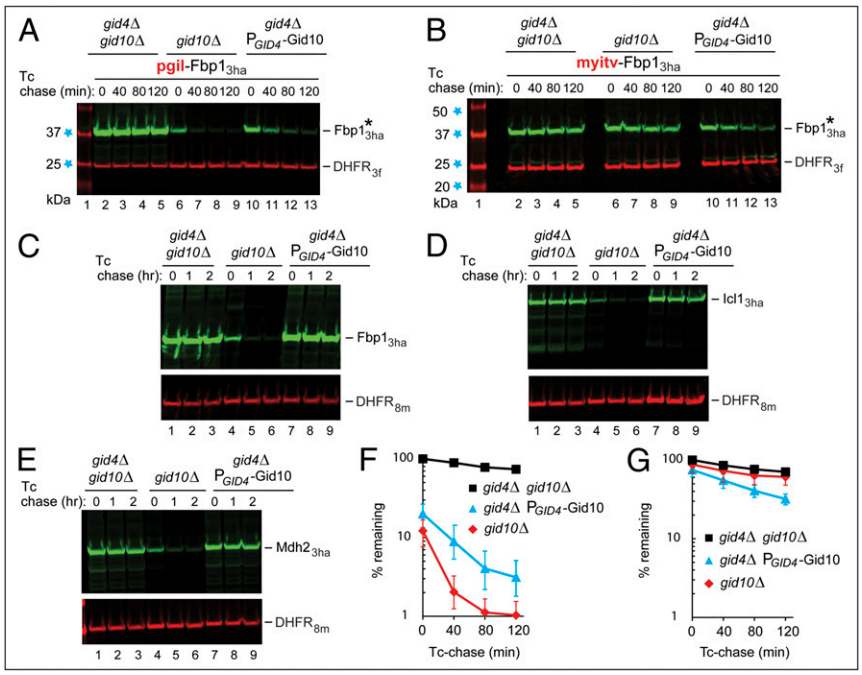

Fig. 3. Chase-degradation assays with gluconeogenic enzymes and other substrates of the GID ubiquitin ligase. Tc-based chases used PRT (see *Materials and Methods*). (*A*) In the pgil-Fbp1$_{3ha}$ test protein, the PTLV Nt-sequence of wild-type Fbp1 was replaced by PGIL, which interacted with both Gid4 and Gid10 (see Fig. 2*B*). Lane 1, M_R markers, indicated on the *Left*. Lanes 2 through 5, pgil-Fbp1$_{3ha}$ in [*gid4Δ gid10Δ*] cells. Lanes 6 through 9, same but in [*gid10Δ*] cells. Lanes 10 through 13, same but in [*gid4Δ* P_{GID4}-*GID10*] cells, which lacked Gid4 and expressed Gid10 from the P_{GID4} promoter. (*B*) Tc/PRT-based degradation assays with myitv-Fbp1$_{3ha}$ (Nt-MYITV interacted with Gid10 but not with Gid4; Fig. 2*B*). Lane 1, M_R markers. Lanes 2 through 5, myitv-Fbp1$_{3ha}$ in [*gid4Δ gid10Δ*] cells. Lanes 6 through 9, same but in [*gid10Δ*] cells. Lanes 10 through 13, same but in [*gid4Δ* P_{GID4}-*GID10*] cells. (*C*) Tc/PRT-based assays with ptlv-Fbp1$_{3ha}$ (wild-type Fbp1), in [*gid4Δ gid10Δ*] cells (lanes 1 through 3), in *gid10Δ* cells (lanes 4 through 6) and in [*gid4Δ* P_{GID4}-*GID10*] cells (lanes 7 through 9). (*D*) Same in *C* but with wild-type (C-terminally triple-ha tagged) Icl1. (*E*) Same as in *C* but with wild-type (C-terminally triple-ha tagged) Mdh2. (*F*) Quantification of data in *A*. (*G*) Quantification of data in *B*. Standard errors were calculated from results of 3 independent Tc/PRT-based degradation assays.

Gluconeogenic Enzymes Are Targeted for Degradation by Gid4, Not by Gid10. Gid10 and Gid4 were found to recognize nonidentical but overlapping sets of Nt-sequence motifs (Fig. 2*B*). We asked, using PRT-based chase-degradation assays and the [*gid4Δ* P_{GID4}-*GID10*] strain (lacking Gid4 and expressing Gid10 from the P_{GID4} promoter), whether C-terminally epitope-tagged Fbp1$_{3ha}$, Mdh2$_{3ha}$, and Icl1$_{3ha}$ might be targeted for degradation by ectopically expressed Gid10 in cells growing in the presence of glucose. The results clearly showed that while Fbp1$_{3ha}$, Mdh2$_{3ha}$, and Icl1$_{3ha}$ were short-lived in Gid4-containing *gid10Δ* cells, these proteins were stable in Gid10-expressing, Gid4-lacking [*gid4Δ* P_{GID4}-*GID10*] cells and also (predictably) in double-mutant [*gid4Δ gid10Δ*] cells (Fig. 3 *C*–*E*). In sum, Gid10 does not significantly contribute to the degradation of Fbp1$_{3ha}$, Mdh2$_{3ha}$, and Icl1$_{3ha}$, even if Gid10 is ectopically expressed under conditions in which Gid4 would mediate such a degradation.

Expression of Gid10 Is Induced by Osmotic Stress or Starvation. To investigate physiological functions of *S. cerevisiae* Gid10, we began by identifying conditions under which the *GID10* gene was expressed. Earlier trancriptome-wide expression studies indicated that osmotic stress and amino acid starvation were two conditions that caused a significant increase in *GID10* (*YGR066C*) mRNA (118–121). However, quantitative assessments of this information in databases were complicated by low levels of *GID10* expression. Therefore, we carried out independent experiments, using reverse transcription of mRNAs followed by quantitative PCR (RT-qPCR). These assays confirmed that *S. cerevisiae GID10* mRNA was transiently induced upon a high-salt (1.4 M NaCl) or sorbitol (1 M) osmotic stress (Fig. 4 *A* and *B*). *GID10* mRNA was also induced upon transition from a medium rich in amino acids (YPD medium) to a minimal medium without amino acids, or upon starvation for individual amino acids (Fig. 4*B*) (see *Materials and Methods*).

To detect expression of the Gid10 protein, we constructed a strain in which Gid10 (expressed from its native P_{GID10} promoter) was tagged with a triple-flag Nt-epitope, yielding a functionally active $_{3f}$Gid10 (*SI Appendix*, Fig. S1). Expression of the $_{3f}$Gid10 protein upon osmotic stress, while functionally relevant, was still too low for detection by a direct immunoblotting (IB). Nevertheless, $_{3f}$Gid10 could be detected after its enrichment on anti-flag beads, followed by its elution from the beads, SDS/PAGE, and IB assays (Fig. 4*C*).

Gid10 Functions as a Part of the GID Ubiquitin Ligase. To address the relevance of Gid10 to protein degradation under conditions in which this protein was naturally expressed, we carried out PRT-based chase-degradation assays with pgil-Fbp1$_{3ha}$ and endogenous Gid10, with the latter naturally expressed during osmotic stress mediated by 1.4 M NaCl. The results showed that under these conditions (in cells that lacked Gid4) Gid10 was expressed at levels sufficient to destabilize pgil-Fbp1$_{3ha}$ (Fig. 5 *C* and *D*). We also found that the Gid10-mediated degradation of pgil-Fbp1$_{3ha}$ in the presence of 1.4 M NaCl required, in addition, the rest of the GID ubiquitin ligase. Specifically, pgil-Fbp1$_{3ha}$ became stable in a double-mutant [*gid2Δ gid4Δ*] strain that lacked not only *GID4* but also *GID2* (46, 86), an essential subunit of GID (Fig. 5 *E* and *G*.).

Additional and independent evidence for a Gid10-GID association was provided by coimmunoprecipitation assays with ha-tagged Gid1$_{3ha}$, an essential subunit of GID (46) and flag-tagged $_{3f}$Gid10 in extracts from *S. cerevisiae* expressing these test proteins. Specifically, immunoprecipitation of $_{3f}$Gid10 with a monoclonal anti-flag antibody coimmunoprecipitated Gid1$_{3ha}$ as well (Fig. 5*A*). We also found that interactions of $_{3f}$Gid10 with Gid1$_{3ha}$ (and, by inference, with the rest of the GID complex) were significantly weakened in the absence the GID subunit Gid5 (in extracts from a [*gid5Δ*] strain) (Fig. 5*A*). An analogous observation of the Gid5 dependence was previously made in regard to interactions between Gid1 and Gid4 (86).

We also verified the binding of Gid10 to its protein substrate using a method other than Y2H. Specifically, in immunoprecipitation assays, $_{3f}$Gid10 was coimmunoprecipitated with pgil-Fbp1$_{3ha}$, an in vivo physical ligand and degradation substrate of Gid10, but not with the otherwise identical test protein sgil-Fbp1$_{3ha}$, in which the Nt-Pro residue was replaced by Nt-Ser (Fig. 5*B*). This requirement for Nt-Pro in a substrate for its binding to Gid10 is analogous to the previously demonstrated requirement for Nt-Pro in the Nt-PTLV sequence of WT Fbp1 for its binding to the Gid4 N-recognin (46).

Gid4, the main N-recognin of the Pro/N-degron pathway, is a short-lived protein. Gid4 is targeted for degradation largely (though not solely) by the GID Ub ligase, of which Gid4 itself is a subunit (86, 97). A GID-recognized degron of Gid4 remains to be identified (Gid4 lacks both Nt-Pro and a Pro at position 2). We found that, analogously to Gid4, the $_{3f}$Gid10 protein was also a short-lived protein that was substantially (but incompletely, similarly to Gid4) stabilized in a [*gid2Δ*] strain that lacks the active GID Ub ligase (Fig. 5*F*). Together, independent lines of evidence described in this study (Figs. 3–5) indicate that when the endogenous Gid10 is naturally expressed, it can function as an alternative N-recognin of the yeast Pro/N-degron pathway, i.e., as a substrate-recognizing subunit of GID. Analogies between GID-associated Gid4 and GID-associated Gid10 include their vulnerability to being targeted for degradation by the GID Ub ligase (Fig. 5*F*).

Gid4 and Gid10 Diverged Early after Genome Duplication in Budding Yeast. Sequelogs (see above, and ref. 112) of the *Sc*-Gid4 protein are present in most eukaryotes, from fungi/yeasts to animals and plants. While some eukaryotic genomes encode 2 Gid4-like proteins, most encode only 1. Between 1×10^7 and 1×10^8 years ago, an ancestor of a set of budding yeast lineages that included ancestors of *S. cerevisiae* and other *Saccharomyces* yeasts underwent a whole genome duplication, probably as a result of interspecies hybridization (122–125). A plausible scenario, therefore, is that *Sc*-Gid4 and *Sc*-Gid10 are descendants of a pair of (initially) identical or nearly identical proteins that underwent a sequence and functional divergence (including divergence in their modes of expression), and became Gid4 and Gid10 of extant *S. cerevisiae*. In agreement with this model, genomes of budding yeasts that did not undergo whole genome duplication contain a single gene encoding a Gid4-like protein.

Fig. 6 describes evolutionary relationships among 20 species of budding yeasts (a subset of "sequenced" budding yeasts), including *Saccharomyces* yeasts (126). All yeasts in Fig. 6 are descendants of the whole genome duplication event. Their genomes encode 1 or 2 proteins that are significantly sequelogous to *Sc*-Gid4/*Sc*-Gid10. Our examination of the predicted amino acid sequences of these proteins (Fig. 6 and *SI Appendix*, Fig. S2) showed that the 20 yeast species could be classed as 3 sets in regard to *Sc*-Gid4/*Sc*-Gid10, as indicated in Fig. 6:

1) Yeasts in which a genome encodes an *Sc*-Gid4–like protein and an *Sc*-Gid10–like protein. *S. cerevisiae* and other indicated *Saccharomyces* yeasts are the sole members of this set (Fig. 6).
2) Non-*Saccharomyces* yeasts in which a genome encodes an *Sc*-Gid4–like protein and also a protein that is sequelogous (to comparable extents) to both *Sc*-Gid4 and *Sc*-Gid10 (Fig. 6).
3) Non-*Saccharomyces* yeasts in which a genome encodes a single *Sc*-Gid4–like protein (Fig. 6).

We conclude that after whole genome duplication, the (eventual) *Sc*-Gid10 protein diverged relatively early from the (eventual) *Sc*-Gid4 protein, and also that only *Saccharomyces* yeasts, the ones that are closely related to *S. cerevisiae*, contain a gene that encodes a clearly identifiable sequelog of the *Sc*-Gid10 protein (Fig. 6). Given these evolutionary patterns, while both Gid4 and Gid10 can function as N-recognins of the GID Ub ligase (see above), it is Gid4 but not Gid10 that is the functionally major and particularly highly conserved N-recognin of the Pro/N-degron pathway (Figs. 1*C*, 2*A*, and 6). A blend of natural selection and quasirandom mutational drift (127) maintained Gid4-like proteins as universally present N-recognins of the Pro/N-degron pathway, whereas unambiguously assignable sequelogs of *Sc*-Gid10 were retained solely within the *Saccharomyces* clade. This conclusion is consistent with expression of *Sc*-Gid4 under a variety of conditions. While the expression of

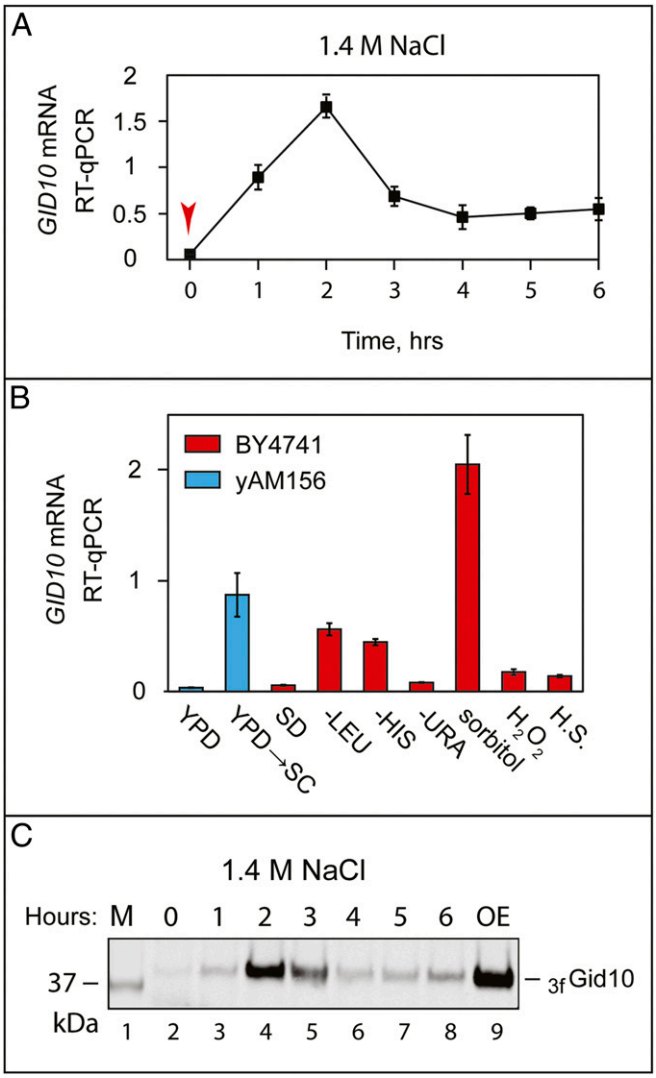

Fig. 4. Expression of *S. cerevisiae GID10* upon specific stresses. (*A*) Osmotic shock was induced by 1.4 M NaCl. BY4741 (*MATa his3 leu2 met15 ura3*) cells in midexponential growth were harvested at 1-h intervals after making the medium 1.4 M in NaCl (time 0; indicated by a red arrowhead), followed by measurements of *GID10* mRNA (relative to 2 unrelated mRNAs) using RT-qPCR (see *Materials and Methods*). (*B*) Changes in the relative levels of *GID10* mRNA were measured in BY4741 cells that had been subjected to a variety of 30-min stresses (red rectangles). Specifically, transitions from a minimal (SD) media containing all required supplements to SD lacking either Leu, or His, or Ura; or a 30-min treatment with 1 M sorbitol in the complete SD; or a 30-min incubation with H_2O_2 (at 0.32 mM) in complete SD; or a 30-min incubation in complete SD at 37 °C (heat stress). Alternatively, a yeast strain with a single auxotrophy (yAM156, *ura3*) was subjected to a transition from a rich (YPD) medium to a minimal medium (SC +Ura) for 30 min (blue rectangles). Standard errors were calculated from results of 3 independent experiments. (*C*) *S. cerevisiae* cells in which the N-terminally triple-flagged Gid10 ($_{3f}$Gid10) was expressed from its endogenous locus and the native P_{GID10} promoter were subjected to osmotic shock with 1.4 M NaCl (*A*). The $_{3f}$Gid10 protein was detected by SDS/PAGE and immunoblotting with anti-flag antibody, after a partial enrichment of samples (uniformly across samples) for $_{3f}$Gid10 using anti-flag beads. Lane 1, a 37-kDa molecular mass marker. Lanes 2 through 8, levels of $_{3f}$Gid10 as a function of time after the addition of NaCl. Lane 9, a sample from cells that overexpressed $_{3f}$Gid10 (see *Materials and Methods*).

Sc-Gid4 was initially presumed to occur largely during a transition from gluconeogenesis to glycolysis, it became clear later that *Sc*-Gid4 is also present, at varying levels, under other conditions as well, including media containing glucose (46). In contrast, the

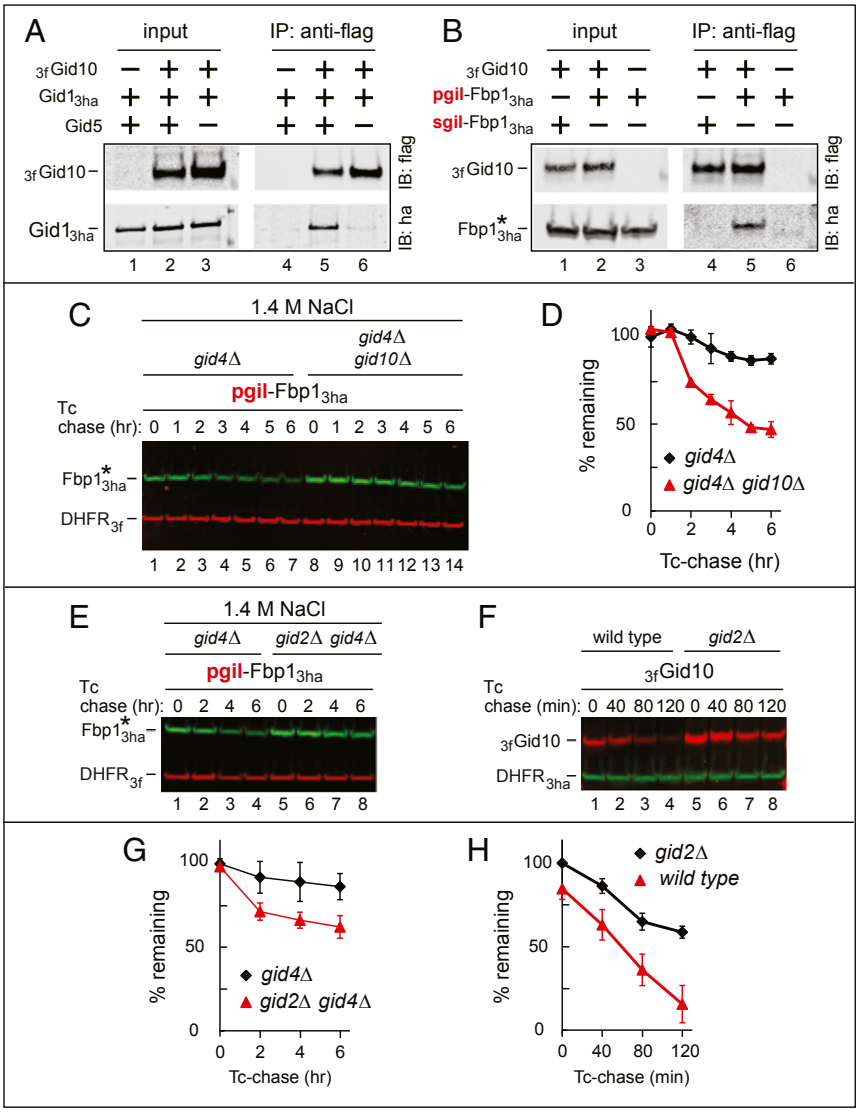

Fig. 5. Gid10-GID interactions and Gid10-mediated protein degradation. (*A*) Yeast extracts containing or lacking $_{3f}$Gid10 and Gid1$_{3ha}$, expressed at endogenous levels in the presence or absence of (untagged) Gid5 were immunoprecipitated with anti-flag antibody (specific for $_{3f}$Gid10), followed by SDS/PAGE and IB with either anti-flag or anti-ha, as indicated. (*B*) Same as in *A*, except that yeast extracts contained or lacked $_{3f}$Gid10 and moderately overexpressed pgil-Fbp1$_{3ha}$ (it interacted with Gid10 in Y2H assays; Fig. 2*B*), or the otherwise identical sgil-Fbp1$_{3ha}$, in which Nt-Pro was replaced by Ser. Immunoprecipitation with anti-flag, followed by SDS/PAGE and IB with either anti-flag or anti-ha, as indicated. (*C*) Tc/PRT-based degradation assays with pgil-Fbp1$_{3ha}$ in cells exposed to 1.4 M NaCl (conditions that induce expression of endogenous Gid10). Lanes 1 through 7, in *gid4*Δ cells. Lanes 8 through 14, in [*gid4*Δ *gid10*Δ] cells. (*D*) Quantification of data in *C*. (*E*) Tc/PRT-based degradation assays with pgil-Fbp1$_{3ha}$ (in the presence of 1.4 M NaCl) in *gid4*Δ cells (lanes 1 through 4) and in [*gid2*Δ *gid4*Δ] cells (lanes 5 through 8). (*F*) Tc/PRT-based degradation assays with $_{3f}$Gid10 in "wild-type" (*GID4 GID10*) cells (lanes 1 through 4) and in *gid10*Δ cells (lanes 5 through 8). (*G*) Quantification of data in *E*. (*H*) Quantification of data in *F*. Standard errors were calculated from results of 3 independent Tc/PRT-based assays.

natural expression of *Sc*-Gid10 is confined to specific stresses (Fig. 4). We also note that the phylogenetic tree of clearly identifiable sequelogs of *Sc*-Gid4 (but not of *Sc*-Gid10) is highly similar to the evolutionary tree of budding yeasts in general.

In sum, a previously uncharacterized *S. cerevisiae* protein (YGR066C), termed Gid10 and sequelogous to the *S. cerevisiae* Gid4 N-recognin of the Pro/N-degron pathway, has been shown here to be naturally expressed under specific conditions such as osmotic stress and starvation, in contrast to the relatively ubiquitously expressed Gid4. Using several experimental strategies, we also showed that the substrate specificity of Gid10 is similar but not identical to that of Gid4, and that Gid10 is a functionally minor but bona fide alternative N-recognin of the Pro/N-degron pathway (Figs. 2–6).

Materials and Methods

Antibodies and Other Reagents. Mouse monoclonal (clone M2) anti-flag antibody (Sigma) was used for immunoblotting and coimmunoprecipitation of flag-tagged proteins. Immunoblotting of ha-tagged proteins was carried out with rabbit polyclonal anti-ha antibody (Sigma), while myc-tagged proteins were detected with mouse monoclonal (clone 9E10) anti–c-myc antibody (Sigma). The following fluorescently labeled secondary antibodies were used for detecting proteins after a Tc/PRT-based chase: IRDye 800 CW goat anti-rabbit IgG and IRDye 680RD goat anti-mouse IgG (LI-COR Biosciences). For detecting proteins after coimmunoprecipitation, we used IRDye 800CW goat anti-rabbit IgG and IRDye 800CW goat anti-mouse IgG. The following medium components were used (they are listed below with their sources in parentheses): yeast nitrogen base with ammonium sulfate (MP Biomedicals); complete supplement mixtures of amino acids for *S. cerevisiae* growth (MP Biomedicals), with appropriate nutrients omitted to maintain marker-bearing plasmids; yeast extract (Difco); yeast peptone (Difco); glucose (Sigma); and tetracycline (Sigma). A variety of restriction enzymes (used for plasmid construction), T4 DNA ligase, and Q5 DNA polymerase were from New England Biolabs.

Yeast Strains and Media. *S. cerevisiae* strains used in this study are described in *SI Appendix*, Table S1. Standard techniques were used for constructing plasmids and yeast strains (*SI Appendix*, Tables S1 and S2) (128). All final DNA constructs were verified by DNA sequencing. With the exception of the *S. cerevisiae* strain (AH109), used for Y2H assays, yeast strains were derived from BY4741 (S288c lineage, *MATa his3Δ1 leu2Δ met15Δ ura3Δ*). New yeast strains were constructed by transformation of the parent strain with PCR products containing short homology regions directed to the locus of interest (129). Yeast cultures were grown either in YPD (1% yeast extract, 2% peptone, 2% glucose), SD (5 g/L ammonium sulfate, 1.7 g/L yeast nitrogen base supplemented with complete amino acid supplement mixture minus appropriate dropouts, 2% glucose), or SC (5 g/L ammonium sulfate, 1.7 g/L yeast nitrogen base, 2% glucose). Yeast shuttle vectors were usually transformed into DH5a competent *Escherichia coli* (Invitrogen). Plasmids used in yeast-based PRT assays were transformed into SURE 2 competent *E. coli* (Agilent Technologies).

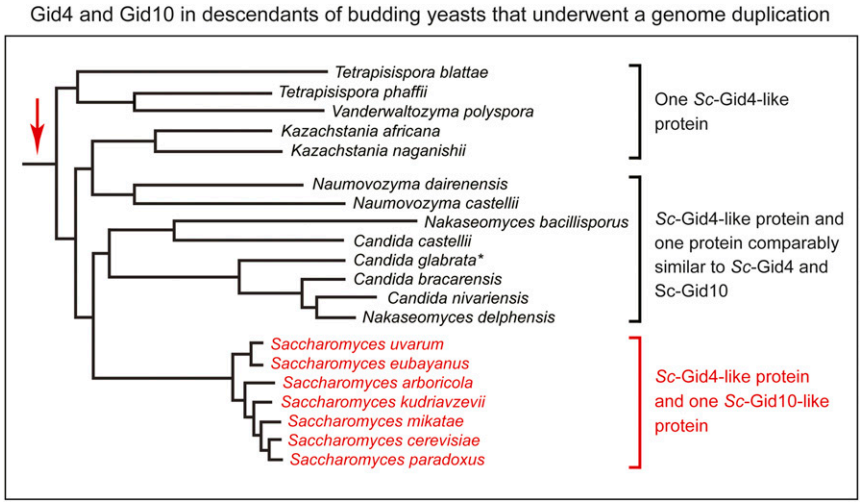

Fig. 6. Gid4, Gid10, and phylogenetic tree of budding yeasts that underwent a whole genome duplication. The latter is indicated by a red arrow on the *Left*. The lengths of horizontal lines are approximately proportional to elapsed times (inferred from coalescence-based analyses) (126) before divergences of indicated yeast species. Alignments of Gid4/Gid10 amino acid sequences encoded by the genomes of these yeasts partitioned them into 3 sets, as indicated on the *Right*. The phylogenetic tree of relevant protein sequences is shown in *SI Appendix*, Fig. S2. The *Saccharomyces* set, in which yeasts contain both an *Sc*-Gid4–like and an *Sc*-Gid10–like protein, is highlighted in red. *Candida glabrata* (indicated by an asterisk) is the only species in its group that contains a single *Sc*-Gid4–like protein.

Y2H Binding Assays and Screening for N-Terminal Gid10-Binding Peptide Motifs. The AH109 yeast strain was used for all Y2H experiments. It was sequentially transformed with pCSJ392 or pCSJ182, followed by transformation with pAM1674 or an analogous plasmid (*SI Appendix*, Table S2). *S. cerevisiae* carrying both plasmids were grown to a near-stationary phase ($OD_{600} \sim 2$; 1 mL of yeast suspension with $OD_{600} = 1$ contains $\sim 10^7$ cells), concentrated by centrifugation, washed, resuspended in PBS buffer, and spotted on SD [−Leu, −Trp, −His] plates (relative dilutions: 2.0, 0.67, 0.22, 0.074, and 0.025). Cultures on plates were imaged after 3 d of growth at 30 °C. To construct Y2H-based Nt-peptide library, termed pAM1160, the Y2H cloning vector pGBKCg (*SI Appendix*, Table S2) was modified by PCR so that the P_{ADH1} promoter was followed by a *Spe*I restriction site, a short linker containing an *Eco*RI site, and ending with a *Xho*I site that is present naturally in the sequence of a segment encoding the Gal4 DBD. A corresponding DNA fragment was cut with *Spe*I and *Xho*I, dephosphorylated, and gel purified. The insert to be ligated into this backbone [*Spe*I-$MX_2X_3X_4X_5$-GGGGGG-Dhfr-Gal4DBD(Nt-half)-*Xho*I] was obtained by PCR using primers 5′-CACAactagtATGNNNNNNNNNNNNggt GGAGGAGGGGGTGGAGTTCG-3′ and 5′-tcttctcgaggaaaaatcagtagaaatagc-3′, and the plasmid pCSJ376 as a template ("N" denotes a mixture of 4 nucleotides). The resulting PCR product was digested with *Spe*I and *Xho*I. Following ligation, the reaction mixture was briefly treated with *Eco*RI to eliminate possible background from undigested vector. Products of ligation were then transformed into DH5a *E. coli*, resulting in ∼16,000 colonies that comprised the library. Colonies were scraped off the plates into PBS buffer, followed by purification of total plasmid DNA using the Maxiprep plasmid isolation kit (Qiagen). We also constructed a similar library (pAM1479) using a primer (5′-CACAactagtATGNDNNNNNNNNNNggt GGAGGAGGGGGTGGAGTTCG-3′) that eliminated Pro (as well as Ala and Thr) from position X_2. For library screening, AH109 yeast cells growing in YPD in early exponential phase were collected by centrifugation (30 mL of yeast suspension with $OD_{600} = 1$; corresponds to $\sim 3 \times 10^8$ cells) and thereafter transformed with 1 μg of the library plasmid. The resulting cells were incubated in a batch culture in SD [−Leu, −Trp] for 1 h and thereafter plated on 2% agar SD[−Leu, −Trp, −His] plates. After 3 d at 30 °C, several positive clones were selected for regrowth on the same medium, plasmid extraction, and retesting in Y2H assays. Those library-derived plasmids that conferred positive Y2H signals upon retesting were analyzed by DNA sequencing.

Tc/PRT Chase-Degradation Assays and Immunoblotting. Tc/PRT protein degradation assays were carried out as described in *Results and Discussion* (20). Briefly, batch yeast cultures were grown to OD_{600} of 1.0 to 1.5, followed by the addition of Tc to the final concentration of 0.5 mM. For those samples in which expression of *GID10* was to be induced, the growth medium was made 1.4 M in NaCl at the time of Tc addition. At indicated time intervals, a volume of cell suspension corresponding to OD_{600} of 1.0 at the beginning of the Tc chase was collected; this volume was kept constant throughout the chase. Cells were collected by centrifugation, resuspended in 1 mL of 1 M NaOH, and incubated at room temperature for 5 min. Cell were again collected by centrifugation (at the top speed in a microcentrifuge for 1 min) and resuspended in 50 μL of buffer HU (8 M urea, 5% SDS, 1 mM EDTA, 0.1 M dithiothreitol, 0.005% bromophenol blue, 0.2 M Tris·HCl, pH 6.8). These protein solutions were incubated at 70 °C for 10 min and fractionated by SDS/PAGE on 4 to 12% NuPAGE Bis-Tris gels with MES running buffer (Thermo Fisher), followed by electroblotting of proteins onto a nitrocellulose membrane. The membrane was blocked with 5% nonfat milk in TBST (0.1% Tween-20, 0.15 M NaCl, 20 mM Tris, pH 7.4) for 1 h at room temperature. Proteins of interest were detected by incubation at 4 °C with primary antibodies overnight. The membrane was then washed 3 times with TBST and probed with secondary antibodies (described above) in TBST-5% nonfat milk for 1 to 4 h. The membrane was washed 3 times with TBST and imaged using the Odyssey 9120 scanner (LI-COR Biotechnologies). Unless stated otherwise, Tc/PRT chases as well as other key experiments were repeated at least twice.

Co-IP. Co-IP experiments with specific subunits of the GID Ub ligase were carried out using yAM182, yAM184, and yAM199 yeast strains (*SI Appendix*, Table S1). Co-IP of Gid10 with its substrate such as pgil-$Fbp1_{3ha}$ was carried out with yAM220 transformed with pAM1830, and yAM231 transformed with pAM1830 or pAM1836 (*SI Appendix*, Table S2). Cell extracts were prepared as previously described (86). Briefly, a 30-mL cell culture was grown in SD medium to OD_{600} of 1.5. Cells were collected by centrifugation and resuspended in 1 mL of buffer P3 (0.1% Triton X-100, 50 mM NaCl, 50 mM NaF, 5 mM EDTA, 50 mM Tris, pH 7.5) supplemented with the protease inhibitor mixture for fungal use (Sigma). The cells were then disrupted by vortexing with lysing matrix C beads (MP Biomedicals) over 20 cycles of 30 s (followed by 30 s on ice). The resulting extracts were centrifuged for 20 min at 12,000 × *g* in a microcentrifuge, and the supernatant was added to the magnetic beads (Dynabeads Protein G [Thermo Fisher] bound to anti-flag antibody described above). The resulting mixtures were incubated with rotation at 4 °C for 2 h, followed by 3 washes with buffer P3 and elution of proteins with HU buffer.

RT-qPCR. It was carried out with RNA samples from BY4741 and yAM156 *S. cerevisiae* strains, as described in *Results and Discussion*. Total RNA from yeast cultures was purified using the Quick-RNA Fungal/Bacterial Miniprep Kit (Zymoresearch), and 500-ng samples of RNA were used in a reverse transcription reaction with NxGen M-MuLV reverse transcriptase (Lucigen) and oligo$(dT)_{18}$ primer. qPCR was then carried out on the resulting cDNA using 2× qPCR master mix without ROX (Bioland Scientific) on a Mastercycler Ep Realplex apparatus (Eppendorf). Two reference yeast genes (*ALG9* and *TAF10*) were used for normalization/calibration of qPCR measurements (130).

Phylogenetic Analyses of Protein Sequences. Amino acid sequences of Gid4-like proteins were obtained from databases of the Y1000+ Project (126). Phylogenetic analyses of these sequences was carried out through the phylogeny.fr pipeline (131, 132) using the "one click" option. Briefly, the sequences were aligned using MUSCLE (133), curated by Gblocks (134), and the phylogenetic tree was built by PhyML (135) and rendered by TreeDYN (136).

ACKNOWLEDGMENTS. We are grateful to the present and former members of the A.V. laboratory for their assistance and advice. This work was supported by grants to A.V. from the National Institutes of Health (GM031530 and DK039520).

1. A. Hershko, A. Ciechanover, A. Varshavsky, The ubiquitin system. *Nat. Med.* **6**, 1073–1081 (2000).
2. A. Varshavsky, N-degron and C-degron pathways of protein degradation. *Proc. Natl. Acad. Sci. U.S.A.* **116**, 358–366 (2019).
3. A. Varshavsky, Discovery of cellular regulation by protein degradation. *J. Biol. Chem.* **283**, 34469–34489 (2008).
4. D. Finley, H. D. Ulrich, T. Sommer, P. Kaiser, The ubiquitin-proteasome system of Saccharomyces cerevisiae. *Genetics* **192**, 319–360 (2012).
5. Y. Ohsumi, Historical landmarks of autophagy research. *Cell Res.* **24**, 9–23 (2014).
6. V. Lahiri, W. D. Hawkins, D. J. Klionsky, Watch what you (self-) eat: Autophagic mechanisms that modulate metabolism. *Cell Metab.* **29**, 803–826 (2019).
7. E. M. Sontag, R. S. Samant, J. Frydman, Mechanisms and functions of spatial protein quality control. *Annu. Rev. Biochem.* **86**, 97–122 (2017).
8. V. Vittal, M. D. Stewart, P. S. Brzovic, R. E. Klevit, Regulating the regulators: Recent revelations in the control of E3 ubiquitin ligases. *J. Biol. Chem.* **290**, 21244–21251 (2015).
9. M. Rape, Ubiquitylation at the crossroads of development and disease. *Nat. Rev. Mol. Cell Biol.* **19**, 59–70 (2018).
10. C. Enam, Y. Geffen, T. Ravid, R. G. Gardner, Protein quality control degradation in the nucleus. *Annu. Rev. Biochem.* **87**, 725–749 (2018).
11. N. Zheng, N. Shabek, Ubiquitin ligases: Structure, function, and regulation. *Annu. Rev. Biochem.* **86**, 129–157 (2017).
12. A. Shiber *et al*., Cotranslational assembly of protein complexes in eukaryotes revealed by ribosome profiling. *Nature* **561**, 268–272 (2018).
13. P. Grumati, I. Dikic, Ubiquitin signaling and autophagy. *J. Biol. Chem.* **293**, 5404–5413 (2018).
14. C. H. Ji, Y. T. Kwon, Crosstalk and interplay between the ubiquitin-proteasome system and autophagy. *Mol. Cells* **40**, 441–449 (2017).
15. S. Shao, R. S. Hegde, Target selection during protein quality control. *Trends Biochem. Sci.* **41**, 124–137 (2016).
16. F. Wang, L. A. Canadeo, J. M. Huibregtse, Ubiquitination of newly synthesized proteins at the ribosome. *Biochimie* **114**, 127–133 (2015).
17. S. A. Comyn, G. T. Chan, T. Mayor, False start: Cotranslational protein ubiquitination and cytosolic protein quality control. *J. Proteomics* **100**, 92–101 (2014).
18. J. Lykke-Andersen, E. J. Bennett, Protecting the proteome: Eukaryotic cotranslational quality control pathways. *J. Cell Biol.* **204**, 467–476 (2014).
19. D. Balchin, M. Hayer-Hartl, F. U. Hartl, In vivo aspects of protein folding and quality control. *Science* **353**, aac4354 (2016).
20. J. H. Oh, S. J. Chen, A. Varshavsky, A reference-based protein degradation assay without global translation inhibitors. *J. Biol. Chem.* **292**, 21457–21465 (2017).
21. G. Kleiger, T. Mayor, Perilous journey: A tour of the ubiquitin-proteasome system. *Trends Cell Biol.* **24**, 352–359 (2014).
22. D. Zattas, M. Hochstrasser, Ubiquitin-dependent protein degradation at the yeast endoplasmic reticulum and nuclear envelope. *Crit. Rev. Biochem. Mol. Biol.* **50**, 1–17 (2015).
23. K. K. Dove, R. E. Klevit, RING-between-RING E3 ligases: Emerging themes amid the variations. *J. Mol. Biol.* **429**, 3363–3375 (2017).
24. C. A. P. Joazeiro, Ribosomal stalling during translation: Providing substrates for ribosome-associated protein quality control. *Annu. Rev. Cell Dev. Biol.* **33**, 343–368 (2017).
25. T. Inobe, S. Fishbain, S. Prakash, A. Matouschek, Defining the geometry of the two-component proteasome degron. *Nat. Chem. Biol.* **7**, 161–167 (2011).
26. N. P. Dantuma, L. C. Bott, The ubiquitin-proteasome system in neurodegenerative diseases: Precipitating factor, yet part of the solution. *Front. Mol. Neurosci.* **7**, 70 (2014).
27. B. A. Schulman, Twists and turns in ubiquitin-like protein conjugation cascades. *Protein Sci.* **20**, 1941–1954 (2011).
28. J. A. M. Bard *et al*., Structure and function of the 26S proteasome. *Annu. Rev. Biochem.* **87**, 697–724 (2018).
29. A. Schweitzer *et al*., Structure of the human 26S proteasome at a resolution of 3.9 Å. *Proc. Natl. Acad. Sci. U.S.A.* **113**, 7816–7821 (2016).
30. D. Finley, X. Chen, K. J. Walters, Gates, channels, and switches: Elements of the proteasome machine. *Trends Biochem. Sci.* **41**, 77–93 (2016).
31. G. A. Collins, A. L. Goldberg, The logic of the 26S proteasome. *Cell* **169**, 792–806 (2017).
32. L. Budenholzer, C. L. Cheng, Y. Li, M. Hochstrasser, Proteasome structure and assembly. *J. Mol. Biol.* **429**, 3500–3524 (2017).
33. D. Gödderz *et al*., Cdc48-independent proteasomal degradation coincides with a reduced need for ubiquitylation. *Sci. Rep.* **5**, 7615 (2015).
34. H. Yu, A. Matouschek, Recognition of client proteins by the proteasome. *Annu. Rev. Biophys.* **46**, 149–173 (2017).
35. B. M. Stadtmueller, C. P. Hill, Proteasome activators. *Mol. Cell* **41**, 8–19 (2011).
36. A. Bachmair, D. Finley, A. Varshavsky, In vivo half-life of a protein is a function of its amino-terminal residue. *Science* **234**, 179–186 (1986).
37. A. Bachmair, A. Varshavsky, The degradation signal in a short-lived protein. *Cell* **56**, 1019–1032 (1989).
38. A. Varshavsky, The N-end rule pathway and regulation by proteolysis. *Protein Sci.* **20**, 1298–1345 (2011).
39. J. W. Tobias, T. E. Shrader, G. Rocap, A. Varshavsky, The N-end rule in bacteria. *Science* **254**, 1374–1377 (1991).
40. H. Rao, F. Uhlmann, K. Nasmyth, A. Varshavsky, Degradation of a cohesin subunit by the N-end rule pathway is essential for chromosome stability. *Nature* **410**, 955–959 (2001).
41. D. A. Dougan, D. Micevski, K. N. Truscott, The N-end rule pathway: From recognition by N-recognins, to destruction by AAA+proteases. *Biochim. Biophys. Acta* **1823**, 83–91 (2012).
42. T. Tasaki, S. M. Sriram, K. S. Park, Y. T. Kwon, The N-end rule pathway. *Annu. Rev. Biochem.* **81**, 261–289 (2012).
43. D. J. Gibbs, J. Bacardit, A. Bachmair, M. J. Holdsworth, The eukaryotic N-end rule pathway: Conserved mechanisms and diverse functions. *Trends Cell Biol.* **24**, 603–611 (2014).
44. N. Dissmeyer, S. Rivas, E. Graciet, Life and death of proteins after protease cleavage: Protein degradation by the N-end rule pathway. *New Phytol.* **218**, 929–935 (2018).
45. M. A. Eldeeb, L. C. A. Leitao, R. P. Fahlman, Emerging branches of the N-end rule pathways are revealing the sequence complexities of N-termini dependent protein degradation. *Biochem. Cell Biol.* **96**, 289–294 (2018).
46. S. J. Chen, X. Wu, B. Wadas, J.-H. Oh, A. Varshavsky, An N-end rule pathway that recognizes proline and destroys gluconeogenic enzymes. *Science* **355**, 366 (2017).
47. C. Dong *et al*., Molecular basis of GID4-mediated recognition of degrons for the Pro/N-end rule pathway. *Nat. Chem. Biol.* **14**, 466–473 (2018).
48. D. A. Dougan, A. Varshavsky, Understanding the Pro/N-end rule pathway. *Nat. Chem. Biol.* **14**, 415–416 (2018).
49. K. I. Piatkov, T. T. Vu, C. S. Hwang, A. Varshavsky, Formyl-methionine as a degradation signal at the N-termini of bacterial proteins. *Microb. Cell* **2**, 376–393 (2015).
50. J. M. Kim *et al*., Formyl-methionine as an N-degron of a eukaryotic N-end rule pathway. *Science* **362**, eaat0174 (2018).
51. M. K. Kim, S. J. Oh, B. G. Lee, H. K. Song, Structural basis for dual specificity of yeast N-terminal amidase in the N-end rule pathway. *Proc. Natl. Acad. Sci. U.S.A.* **113**, 12438–12443 (2016).
52. T. Szoradi *et al*., SHRED is a regulatory cascade that reprograms Ubr1 substrate specificity for enhanced protein quality control during stress. *Mol. Cell* **70**, 1025–1037.e5 (2018).
53. C. S. Hwang, A. Shemorry, A. Varshavsky, N-terminal acetylation of cellular proteins creates specific degradation signals. *Science* **327**, 973–977 (2010).
54. H. K. Kim *et al*., The N-terminal methionine of cellular proteins as a degradation signal. *Cell* **156**, 158–169 (2014).
55. R.-G. Hu *et al*., The N-end rule pathway as a nitric oxide sensor controlling the levels of multiple regulators. *Nature* **437**, 981–986 (2005).
56. S. T. Kim *et al*., The N-recognin UBR4 of the N-end rule pathway is required for neurogenesis and homeostasis of cell surface proteins. *PLoS One* **13**, e0202260 (2018).
57. K. T. Nguyen *et al*., N-terminal acetylation and the N-end rule pathway control degradation of the lipid droplet protein PLIN2. *J. Biol. Chem.* **294**, 379–388 (2019).
58. A. Shemorry, C. S. Hwang, A. Varshavsky, Control of protein quality and stoichiometries by N-terminal acetylation and the N-end rule pathway. *Mol. Cell* **50**, 540–551 (2013).
59. B. Wadas *et al*., Degradation of serotonin N-acetyltransferase, a circadian regulator, by the N-end rule pathway. *J. Biol. Chem.* **291**, 17178–17196 (2016).
60. B. Wadas, K. I. Piatkov, C. S. Brower, A. Varshavsky, Analyzing N-terminal arginylation through the use of peptide arrays and degradation assays. *J. Biol. Chem.* **291**, 20976–20992 (2016).
61. M. M. Rinschen *et al*., The ubiquitin ligase Ubr4 controls stability of podocin/MEC-2 supercomplexes. *Hum. Mol. Genet.* **25**, 1328–1344 (2016).
62. R. F. Shearer, M. Iconomou, C. K. Watts, D. N. Saunders, Functional roles of the E3 ubiquitin ligase UBR5 in cancer. *Mol. Cancer Res.* **13**, 1523–1532 (2015).
63. J. E. Flack, J. Mieszczanek, N. Novcic, M. Bienz, Wnt-dependent inactivation of the Groucho/TLE co-repressor by the HECT E3 ubiquitin ligase Hyd/UBR5. *Mol. Cell* **67**, 181–193.e5 (2017).
64. J. H. Oh, J. Y. Hyun, A. Varshavsky, Control of Hsp90 chaperone and its clients by N-terminal acetylation and the N-end rule pathway. *Proc. Natl. Acad. Sci. U.S.A.* **114**, E4370–E4379 (2017).
65. E. Graciet *et al*., Aminoacyl-transferases and the N-end rule pathway in a human pathogen. *Proc. Natl. Acad. Sci. U.S.A.* **103**, 3078–3083 (2006).
66. R. Schmidt, R. Zahn, B. Bukau, A. Mogk, ClpS is the recognition component for Escherichia coli substrates of the N-end rule degradation pathway. *Mol. Microbiol.* **72**, 506–517 (2009).
67. I. Rivera-Rivera, G. Román-Hernández, R. T. Sauer, T. A. Baker, Remodeling of a delivery complex allows ClpS-mediated degradation of N-degron substrates. *Proc. Natl. Acad. Sci. U.S.A.* **111**, E3853–E3859 (2014).
68. S. M. Shim *et al*., The endoplasmic reticulum-residing chaperone BiP is short-lived and metabolized through N-terminal arginylation. *Sci. Signal.* **11**, eaan0630 (2018).
69. Y. D. Yoo *et al*., N-terminal arginylation generates a bimodal degron that modulates autophagic proteolysis. *Proc. Natl. Acad. Sci. U.S.A.* **115**, E2716–E2724 (2018).
70. S. Sekine, R. J. Youle, PINK1 import regulation; a fine system to convey mitochondrial stress to the cytosol. *BMC Biol.* **16**, 2 (2018).
71. B. P. Weaver, Y. M. Weaver, S. Mitani, M. Han, Coupled caspase and N-end rule ligase activities allow recognition and degradation of pluripotency factor LIN-28 during non-apoptotic development. *Dev. Cell* **41**, 665–673.e6 (2017).
72. K. Kitamura, H. Fujiwara, The type-2 N-end rule peptide recognition activity of Ubr11 ubiquitin ligase is required for the expression of peptide transporters. *FEBS Lett.* **587**, 214–219 (2013).
73. J. Vicente *et al*., The Cys-Arg/N-end rule pathway is a general sensor of abiotic stress in flowering plants. *Curr. Biol.* **27**, 3183–3190.e4 (2017).
74. H. Aksnes, A. Drazic, M. Marie, T. Arnesen, First things first: Vital protein marks by N-terminal acetyltransferases. *Trends Biochem. Sci.* **41**, 746–760 (2016).
75. J. Vicente *et al*., Distinct branches of the N-end rule pathway modulate the plant immune response. *New Phytol.* **221**, 988–1000 (2019).

76. K. I. Piatkov, C. S. Brower, A. Varshavsky, The N-end rule pathway counteracts cell death by destroying proapoptotic protein fragments. *Proc. Natl. Acad. Sci. U.S.A.* **109**, E1839–E1847 (2012).
77. K. I. Piatkov, L. Colnaghi, M. Békés, A. Varshavsky, T. T. Huang, The auto-generated fragment of the Usp1 deubiquitylase is a physiological substrate of the N-end rule pathway. *Mol. Cell* **48**, 926–933 (2012).
78. K. I. Piatkov, J.-H. Oh, Y. Liu, A. Varshavsky, Calpain-generated natural protein fragments as short-lived substrates of the N-end rule pathway. *Proc. Natl. Acad. Sci. U.S.A.* **111**, E817–E826 (2014).
79. C. S. Brower, K. I. Piatkov, A. Varshavsky, Neurodegeneration-associated protein fragments as short-lived substrates of the N-end rule pathway. *Mol. Cell* **50**, 161–171 (2013).
80. D. Justa-Schuch *et al*., DPP9 is a novel component of the N-end rule pathway targeting the tyrosine kinase Syk. *eLife* **5**, e16370 (2016).
81. K. T. Nguyen, J. M. Kim, S. E. Park, C. S. Hwang, N-terminal methionine excision of proteins creates tertiary destabilizing N-degrons of the Arg/N-end rule pathway. *J. Biol. Chem.* **294**, 4464–4476 (2019).
82. B. Braun *et al*., Gid9, a second RING finger protein contributes to the ubiquitin ligase activity of the Gid complex required for catabolite degradation. *FEBS Lett.* **585**, 3856–3861 (2011).
83. C. R. Brown, A. B. Wolfe, D. Cui, H. L. Chiang, The vacuolar import and degradation pathway merges with the endocytic pathway to deliver fructose-1,6-bisphosphatase to the vacuole for degradation. *J. Biol. Chem.* **283**, 26116–26127 (2008).
84. G.-C. Hung, C. R. Brown, A. B. Wolfe, J. Liu, H.-L. Chiang, Degradation of the gluconeogenic enzymes fructose-1,6-bisphosphatase and malate dehydrogenase is mediated by distinct proteolytic pathways and signaling events. *J. Biol. Chem.* **279**, 49138–49150 (2004).
85. J. Juretschke, R. Menssen, A. Sickmann, D. H. Wolf, The Hsp70 chaperone Ssa1 is essential for catabolite induced degradation of the gluconeogenic enzyme fructose-1,6-bisphosphatase. *Biochem. Biophys. Res. Commun.* **397**, 447–452 (2010).
86. R. Menssen *et al*., Exploring the topology of the Gid complex, the E3 ubiquitin ligase involved in catabolite-induced degradation of gluconeogenic enzymes. *J. Biol. Chem.* **287**, 25602–25614 (2012).
87. J. Regelmann *et al*., Catabolite degradation of fructose-1,6-bisphosphatase in the yeast Saccharomyces cerevisiae: A genome-wide screen identifies eight novel GID genes and indicates the existence of two degradation pathways. *Mol. Biol. Cell* **14**, 1652–1663 (2003).
88. O. Santt *et al*., The yeast GID complex, a novel ubiquitin ligase (E3) involved in the regulation of carbohydrate metabolism. *Mol. Biol. Cell* **19**, 3323–3333 (2008).
89. T. Schüle, M. Rose, K. D. Entian, M. Thumm, D. H. Wolf, Ubc8p functions in catabolite degradation of fructose-1, 6-bisphosphatase in yeast. *EMBO J.* **19**, 2161–2167 (2000).
90. A. A. Alibhoy, H. L. Chiang, Vacuole import and degradation pathway: Insights into a specialized autophagy pathway. *World J. Biol. Chem.* **2**, 239–245 (2011).
91. A. A. Alibhoy, B. J. Giardina, D. D. Dunton, H. L. Chiang, Vps34p is required for the decline of extracellular fructose-1,6-bisphosphatase in the vacuole import and degradation pathway. *J. Biol. Chem.* **287**, 33080–33093 (2012).
92. A. A. Alibhoy, B. J. Giardina, D. D. Dunton, H. L. Chiang, Vid30 is required for the association of Vid vesicles and actin patches in the vacuole import and degradation pathway. *Autophagy* **8**, 29–46 (2012).
93. H. L. Chiang, R. Schekman, Regulated import and degradation of a cytosolic protein in the yeast vacuole. *Nature* **350**, 313–318 (1991).
94. B. J. Giardina, B. A. Stanley, H. L. Chiang, Comparative proteomic analysis of transition of saccharomyces cerevisiae from glucose-deficient medium to glucose-rich medium. *Proteome Sci.* **10**, 40 (2012).
95. M. Hoffman, H. L. Chiang, Isolation of degradation-deficient mutants defective in the targeting of fructose-1,6-bisphosphatase into the vacuole for degradation in Saccharomyces cerevisiae. *Genetics* **143**, 1555–1566 (1996).
96. H. Liu, T. Pfirrmann, The gid-complex: An emerging player in the ubiquitin ligase league. *Biol. Chem.* 10.1515/hsz-2019-0139 (2019).
97. R. Menssen, K. Bui, D. H. Wolf, Regulation of the Gid ubiquitin ligase recognition subunit Gid4. *FEBS Lett.* **592**, 3286–3294 (2018).
98. B. J. Giardina, H. L. Chiang, Fructose-1,6-bisphosphatase, malate dehydrogenase, isocitrate lyase, phosphoenolpyruvate carboxykinase, glyceraldehyde-3-phosphate dehydrogenase, and cyclophilin A are secreted in Saccharomyces cerevisiae grown in low glucose. *Commun. Integr. Biol.* **6**, e27216 (2013).
99. P. H. Huang, H. L. Chiang, Identification of novel vesicles in the cytosol to vacuole protein degradation pathway. *J. Cell Biol.* **136**, 803–810 (1997).
100. H. L. Shieh, Y. Chen, C. R. Brown, H. L. Chiang, Biochemical analysis of fructose-1,6-bisphosphatase import into vacuole import and degradation vesicles reveals a role for UBC1 in vesicle biogenesis. *J. Biol. Chem.* **276**, 10398–10406 (2001).
101. M. C. Chiang, H. L. Chiang, Vid24p, a novel protein localized to the fructose-1, 6-bisphosphatase-containing vesicles, regulates targeting of fructose-1,6-bisphosphatase from the vesicles to the vacuole for degradation. *J. Cell Biol.* **140**, 1347–1356 (1998).
102. N. Kobayashi *et al*., RanBPM, Muskelin, p48EMLP, p44CTLH, and the armadillo-repeat proteins ARMC8alpha and ARMC8beta are components of the CTLH complex. *Gene* **396**, 236–247 (2007).
103. O. Francis, F. Han, J. C. Adams, Molecular phylogeny of a RING E3 ubiquitin ligase, conserved in eukaryotic cells and dominated by homologous components, the muskelin/RanBPM/CTLH complex. *PLoS One* **8**, e75217 (2013).
104. T. Pfirrmann *et al*., RMND5 from Xenopus laevis is an E3 ubiquitin-ligase and functions in early embryonic forebrain development. *PLoS One* **10**, e0120342 (2015).
105. F. Lampert *et al*., The multi-subunit GID/CTLH E3 ubiquitin ligase promotes cell proliferation and targets the transcription factor Hbp1 for degradation. *eLife* **7**, e35528 (2018).
106. O. Francis, G. E. Baker, P. R. Race, J. C. Adams, Studies of recombinant TWA1 reveal constitutive dimerization. *Biosci. Rep.* **37**, BSR20160401 (2017).
107. Y. Chang *et al*., RanBPM regulates the progression of neuronal precursors through M-phase at the surface of the neocortical ventricular zone. *Dev. Neurobiol.* **70**, 1–15 (2010).
108. X. Jin *et al*., MAGE-TRIM28 complex promotes the Warburg effect and hepatocellular carcinoma progression by targeting FBP1 for degradation. *Oncogenesis* **6**, e312 (2017).
109. L. C. Leal-Esteban, B. Rothé, S. Fortier, M. Isenschmid, D. B. Constam, Role of Bicaudal C1 in renal gluconeogenesis and its novel interaction with the CTLH complex. *PLoS Genet.* **14**, e1007487 (2018).
110. K. Boldt *et al*.; UK10K Rare Diseases Group, An organelle-specific protein landscape identifies novel diseases and molecular mechanisms. *Nat. Commun.* **7**, 11491 (2016).
111. Y. Texier *et al*., Elution profile analysis of SDS-induced subcomplexes by quantitative mass spectrometry. *Mol. Cell. Proteomics* **13**, 1382–1391 (2014).
112. A. Varshavsky, 'Spalog' and 'sequelog': Neutral terms for spatial and sequence similarity. *Curr. Biol.* **14**, R181–R183 (2004).
113. M. Vidal, S. Fields, The yeast two-hybrid assay: Still finding connections after 25 years. *Nat. Methods* **11**, 1203–1206 (2014).
114. A. Brückner, C. Polge, N. Lentze, D. Auerbach, U. Schlattner, Yeast two-hybrid, a powerful tool for systems biology. *Int. J. Mol. Sci.* **10**, 2763–2788 (2009).
115. T. Stellberger *et al*., Improving the yeast two-hybrid system with permutated fusions proteins: The Varicella Zoster Virus interactome. *Proteome Sci.* **8**, 8 (2010).
116. F. Frottin *et al*., The proteomics of N-terminal methionine cleavage. *Mol. Cell. Proteomics* **5**, 2336–2349 (2006).
117. Q. Xiao, F. Zhang, B. A. Nacev, J. O. Liu, D. Pei, Protein N-terminal processing: Substrate specificity of Escherichia coli and human methionine aminopeptidases. *Biochemistry* **49**, 5588–5599 (2010).
118. A. P. Gasch *et al*., Genomic expression programs in the response of yeast cells to environmental changes. *Mol. Biol. Cell* **11**, 4241–4257 (2000).
119. T. Bose *et al*., Cohesin proteins promote ribosomal RNA production and protein translation in yeast and human cells. *PLoS Genet.* **8**, e1002749 (2012).
120. H. C. Causton *et al*., Remodeling of yeast genome expression in response to environmental changes. *Mol. Biol. Cell* **12**, 323–337 (2001).
121. K. Waern, M. Snyder, Extensive transcript diversity and novel upstream open reading frame regulation in yeast. *G3 (Bethesda)* **3**, 343–352 (2013).
122. T. Rolland, B. Dujon, Yeasty clocks: Dating genomic changes in yeasts. *C. R. Biol.* **334**, 620–628 (2011).
123. B. Dujon, Yeast evolutionary genomics. *Nat. Rev. Genet.* **11**, 512–524 (2010).
124. M. Marcet-Houben, T. Gabaldón, Beyond the whole-genome duplication: Phylogenetic evidence for an ancient interspecies hybridization in the baker's yeast lineage. *PLoS Biol.* **13**, e1002220 (2015).
125. M. Kellis, B. W. Birren, E. S. Lander, Proof and evolutionary analysis of ancient genome duplication in the yeast Saccharomyces cerevisiae. *Nature* **428**, 617–624 (2004).
126. X. X. Shen *et al*., Reconstructing the backbone of the Saccharomycotina yeast phylogeny using genome-scale data. *G3 (Bethesda)* **6**, 3927–3939 (2016).
127. M. Lynch, *The Origins of Genome Architecture* (Sinauer Associates, Inc., Sunderland, MA, 2007).
128. F. M. Ausubel *et al*., *Current Protocols in Molecular Biology* (Wiley-Interscience, New York, 2017).
129. D. M. Becker, V. Lundblad, Introduction of DNA into yeast cells. *Curr. Protoc. Mol. Biol.* **27**, 13.7.1–13.7.10 (1993).
130. M. A. Teste, M. Duquenne, J. M. François, J. L. Parrou, Validation of reference genes for quantitative expression analysis by real-time RT-PCR in Saccharomyces cerevisiae. *BMC Mol. Biol.* **10**, 99 (2009).
131. A. Dereeper *et al*., Phylogeny.fr: Robust phylogenetic analysis for the non-specialist. *Nucleic Acids Res.* **36**, W465–W469 (2008).
132. A. Dereeper, S. Audic, J. M. Claverie, G. Blanc, BLAST-EXPLORER helps you building datasets for phylogenetic analysis. *BMC Evol. Biol.* **10**, 8 (2010).
133. R. C. Edgar, MUSCLE: A multiple sequence alignment method with reduced time and space complexity. *BMC Bioinformatics* **5**, 113 (2004).
134. J. Castresana, Selection of conserved blocks from multiple alignments for their use in phylogenetic analysis. *Mol. Biol. Evol.* **17**, 540–552 (2000).
135. S. Guindon, O. Gascuel, A simple, fast, and accurate algorithm to estimate large phylogenies by maximum likelihood. *Syst. Biol.* **52**, 696–704 (2003).
136. F. Chevenet, C. Brun, A. L. Bañuls, B. Jacq, R. Christen, TreeDyn: Towards dynamic graphics and annotations for analyses of trees. *BMC Bioinformatics* **7**, 439 (2006).